

Interaction of antitumor drug $\text{Sn}(\text{CH}_3)_2\text{Cl}_2$ with DNA and RNA

Shohreh Nafisi^{a,*}, Amir Sobhanmanesh^b, Majid Esm-Hosseini^b,
Kamran Alimghaddam^c, Heidar Ali Tajmir-Riahi^d

^aDepartment of Chemistry, Azad University, Tehran Central Branch, Tehran 14169 63316, Iran

^bDepartment of Chemistry, Urumieh University, Urumieh, Iran

^cHematology, Oncology and BMT research Center, Tehran University of Medical Science, Shariati Hospital, Kargar Ave., Tehran 14117 13131, Iran

^dDepartment of Chemistry-Biology, University of Quebec at Trois-Rivieres, C. P. 500, TR, Que., Canada G9A 5H7

Received 2 March 2005; revised 16 April 2005; accepted 19 April 2005

Available online 31 May 2005

Abstract

$\text{Sn}(\text{CH}_3)_2\text{Cl}_2$ exerts its antitumor activity in a specific way. Unlike anticancer $\text{cis-Pt}(\text{NH}_3)_2\text{Cl}_2$ drug which binds strongly to the nitrogen atoms of DNA bases, $\text{Sn}(\text{CH}_3)_2\text{Cl}_2$ shows no major affinity towards base binding. Thus, the mechanism of action by which tinorganometallic compounds exert antitumor activity would be different from that of the cisplatin drug. The aim of this study was to examine the binding of $\text{Sn}(\text{CH}_3)_2\text{Cl}_2$ with calf thymus DNA and yeast RNA in aqueous solutions at pH 7.1–6.6 with constant concentrations of DNA and RNA and various molar ratios of $\text{Sn}(\text{CH}_3)_2\text{Cl}_2/\text{DNA}$ (phosphate) and $\text{Sn}(\text{CH}_3)_2\text{Cl}_2/\text{RNA}$ of 1/40, 1/20, 1/10, 1/5. Fourier transform infrared (FTIR) and UV–visible difference spectroscopic methods were used to determine the $\text{Sn}(\text{CH}_3)_2\text{Cl}_2$ binding mode, binding constant, sequence selectivity and structural variations of $\text{Sn}(\text{CH}_3)_2\text{Cl}_2/\text{DNA}$ and $\text{Sn}(\text{CH}_3)_2\text{Cl}_2/\text{RNA}$ complexes in aqueous solution. $\text{Sn}(\text{CH}_3)_2\text{Cl}_2$ hydrolyzes in water to give $\text{Sn}(\text{CH}_3)_2(\text{OH})_2$ and $[\text{Sn}(\text{CH}_3)_2(\text{OH})(\text{H}_2\text{O})_n]^+$ species. Spectroscopic evidence showed that interaction occurred mainly through $(\text{CH}_3)_2\text{Sn}(\text{IV})$ hydroxide and polynucleotide backbone phosphate group with overall binding constant of $K(\text{Sn}(\text{CH}_3)_2\text{Cl}_2\text{–DNA}) = 1.47 \times 10^5 \text{ M}^{-1}$ and $K(\text{Sn}(\text{CH}_3)_2\text{Cl}_2\text{–RNA}) = 7.33 \times 10^5 \text{ M}^{-1}$. $\text{Sn}(\text{CH}_3)_2\text{Cl}_2$ induced no biopolymer conformational changes with DNA remaining in the B-family structure and RNA in A-conformation upon drug complexation.

© 2005 Elsevier B.V. All rights reserved.

Keywords: DNA; RNA; Drug; Sn cation; Binding constant; Conformation; FTIR; UV–Visible spectroscopy

1. Introduction

It is well known that organotin(IV) compounds display strong biological activity. An overview of organotin chemistry is recently reported and their antitumor activities have been discussed [1,2]. They are known to exert therapeutic effects on various tumor cells [3]. Diorganotin(IV) derivatives and mainly those of dialkyltin(IV) appear to be the most effective [4,5]. The biological and anticancer activities of organotin compounds have been studied by Saxena in 1989 [1]. The activity of a wide range of bioorganotin(IV) compounds were investigated by Molloy [6]. The applications of tin and tin organometallic compounds in pharmacy were studied by Tsangoris and Williams [7].

Sugar-organotin(IV) cation complexation discussed by Nagy et al. [8–10].

The mechanism of biological action of organotin(IV) complexes has not yet been fully understood and being the subject of much controversy. Several studies have been reported on the interaction of tin complexes with DNA by a number of different techniques [3,11,12]. The results of Tin-119 Mossbauer titration of dimethyl(IV)tin hydroxide with DNA showed that the bases and phosphodiester groups of DNA do not exhibit consistent affinity for the tin cation in $\text{SnMe}_2(\text{OH})_2$ which is formed at physiological pH [13,14]. Further, Mossbauer spectroscopy for $\text{Sn}^{\text{IV}}\text{R}_n\text{–DNA}$ condensates confirmed bidentate coordination of the phosphate groups and the formation of mixed hydroxo complexes in the weakly acidic, neutral and strongly basic pH ranges. Two vicinal phosphodiester groups (from DNA duplex) were cis-coordinated and gave an octahedral geometry for Sn cation [15]. The coordination of $\text{Me}_2\text{Sn}(\text{IV})$ to mononucleotides showed direct Sn-phosphate binding and no direct Sn-base interaction [16]. The UV and circular

* Corresponding author. Tel.: +98 21 2408164; fax: +98 21 2408164.
E-mail address: drshohreh@yahoo.com (Sh. Nafisi).

dichroism spectra of Me_2SnCl_2 solution added to calf thymus DNA at neutral pH suggested cation binding to phosphodiester residue, with no alteration of DNA conformation [17]. The ^{31}P -NMR results demonstrated that phosphate groups of DNA act as binding sites for dimethyltin(IV) between pH 4.5 and 7 [3,18]. However, there has been no report on the interaction of tin or organotin complexes with RNA in aqueous solution. Therefore, it was of interest to examine the binding of $\text{Sn}(\text{CH}_3)_2\text{Cl}_2$ to DNA and RNA bases and the backbone phosphate group. FTIR and UV–Visible spectroscopic methods were often used to characterize the nature of drug–DNA and drug–RNA interactions [19–21].

We now report a comparative study of DNA and RNA interactions with $\text{Sn}(\text{CH}_3)_2\text{Cl}_2$ in aqueous solution using different cation concentrations (0.3–12.5 mM) with DNA or RNA concentration of 6.25 mM. Fourier transform infrared (FTIR) and UV–Visible spectroscopic methods were used to obtain structural information regarding the cation binding mode, apparent binding constant, and the effects of cation complexation on the biopolymer secondary structure.

2. Experimental

2.1. Materials and methods

Highly polymerized type I Calf thymus DNA sodium salt (7% Na content) was purchased from Sigma Chemical Co. and was deproteinated by the addition of CHCl_3 and isoamyl alcohol in NaCl solution. Baker yeast RNA sodium salt was purchased from Sigma and used as supplied. $\text{Sn}(\text{CH}_3)_2\text{Cl}_2$ was from Merck Company. Other chemicals were of reagent grade.

2.2. Preparation of stock solutions

Na–DNA or Na–RNA were dissolved to 0.5% w/w, 12.5 mM DNA (phosphate) in water solution at 5 °C for 24 h with occasional stirring to ensure formation of homogeneous solution. The solutions of $\text{Sn}(\text{CH}_3)_2\text{Cl}_2$ at different concentrations (2.5, 1.25, 0.625, 0.312 mM) were also prepared. Mixtures of drug and polynucleotides were prepared by adding $\text{Sn}(\text{CH}_3)_2\text{Cl}_2$ dropwise to the polynucleotide solutions with constant stirring to give the desired drug/polynucleotide(P) molar ratios of 1/40, 1/20, 1/10, and 1/5 at a final DNA and RNA concentration of 0.25% w/w or 6.25 mM DNA(phosphate) or RNA(phosphate). Solution pH was adjusted between 6 and 7 with NaOH solution (0.1 M). The IR spectra were recorded 3 h after initial mixing of drug and polynucleotide solutions. The drug molar ratio more than 1/5 causes DNA gel formation and precipitation.

The absorption spectra were recorded on a LKB model 4054 UV-VIS spectrometer, using various $\text{Sn}(\text{CH}_3)_2\text{Cl}_2$ concentrations of 5 μM to 0.05 mM with final DNA(P) and RNA concentration of 0.1 mM.

Infrared spectra were recorded on a Thermo Nicolet NEXUS model 870 FTIR with a DTGS detector and KBr beam splitter. Solution spectra were taken using AgBr windows with resolution of 4 cm^{-1} and 128 scans. Each set of infrared spectra was taken (three times). The water subtraction was carried out with 0.1 mM NaCl solution used as a reference at pH 6.5–7.5 [22]. A good subtraction was achieved as shown by a flat baseline around 2200 cm^{-1} where the water combination mode is located. The spectra were analyzed with OMNIC software. The FTIR difference spectra [(DNA solution + drug solution) – (DNA solution)] and [(RNA solution + drug solution) – (RNA solution)] were produced, using the bands at 968 cm^{-1} for DNA and 862 cm^{-1} for RNA as internal references. The vibrations at 968 (DNA) and 862 cm^{-1} (RNA) are due to the sugar C–C and sugar phosphate stretching modes and show no spectral changes upon $\text{Sn}(\text{CH}_3)_2\text{Cl}_2$ complexation. These intensity ratios were used to determine drug binding to DNA and RNA bases or the backbone phosphate groups. Similar intensity variations have been used to determine the drug binding to DNA and RNA bases and the backbone phosphate groups [23,24].

3. Results and discussion

3.1. FTIR spectra of $\text{Sn}(\text{CH}_3)_2\text{Cl}_2$ –DNA complexes

The infrared spectral features related to this discussion are presented in Fig. 1. Intensity ratio variations for several DNA in-plane vibrations as a function of $\text{Sn}(\text{CH}_3)_2\text{Cl}_2$ concentrations are shown in Fig. 2A. Evidence for drug binding to A–T, G–C or phosphate comes from spectral changes in DNA in-plane vibrations at 1710 (G, T; mainly guanine), 1662 (T, G, A, C; mainly thymine), 1610 (A, C; mainly adenine), 1492 (C, G; mainly cytosine), 1226 (PO_2 asymmetric) and 1088 cm^{-1} (PO_2 symmetric) [23–30].

At $r=1/40$, decrease of intensity was observed for the guanine band at 1710 (20%), thymine at 1662 (25%), adenine at 1610 (50%), cytosine at 1492 (20%), PO_2 asymmetric at 1226 (20%) and symmetric at 1088 cm^{-1} (20%), upon addition of $\text{Sn}(\text{CH}_3)_2\text{Cl}_2$ (Fig. 2A). However, no major shifting was observed for these vibrations on cation interaction ($\Delta\nu=2 \text{ cm}^{-1}$) (Fig. 1). The observed spectral changes are due to DNA aggregation in the presence of organotinhydroxo complexes. Cation binding to DNA bases and the phosphate group causes major increase of intensity and shifting of these vibrations, while the loss of intensity has been attributed to DNA aggregation, condensation or helix stabilization [29–31].

As $\text{Sn}(\text{CH}_3)_2\text{Cl}_2$ concentration increased ($r=1/20$ and 1/10), the guanine band at 1710 gained minor intensity (10%) (Fig. 2A). Similar intensity increase was also observed for the thymine band at 1662 (13%) and adenine band at 1609 cm^{-1} (15%) and cytosine band at 1492 cm^{-1} (10%) (Fig. 2A). The asymmetric phosphate vibration at

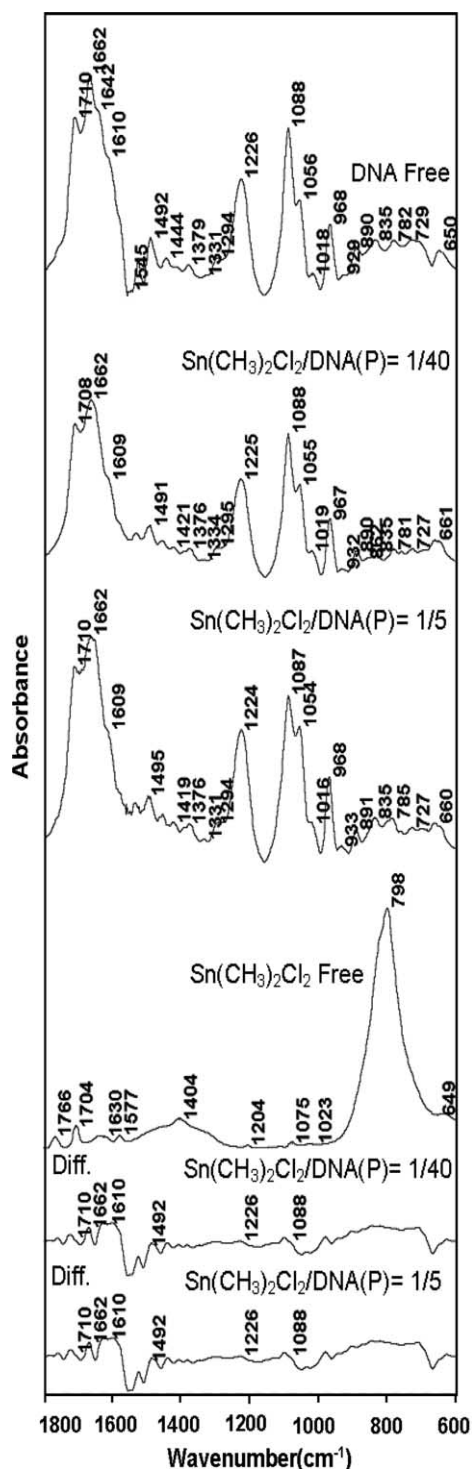


Fig. 1. FTIR spectra in the region of 1800–600 cm^{-1} for free calf-thymus DNA and free $\text{Sn}(\text{CH}_3)_2\text{Cl}_2$, and $\text{Sn}(\text{CH}_3)_2\text{Cl}_2$ –DNA adducts in aqueous solution at pH 6.5–7.5 (top four spectra) and difference spectra for $\text{Sn}(\text{CH}_3)_2\text{Cl}_2$ –DNA adducts obtained at various $\text{Sn}(\text{CH}_3)_2\text{Cl}_2$ –DNA (phosphate) molar ratios (bottom two spectra).

1226 cm^{-1} shifted to 1225 cm^{-1} and exhibited intensity increase (20%) together with the symmetric PO_2 vibration at 1088 cm^{-1} with increase in intensity (15%) (this increase in intensity was compared with the intensity of the bands at

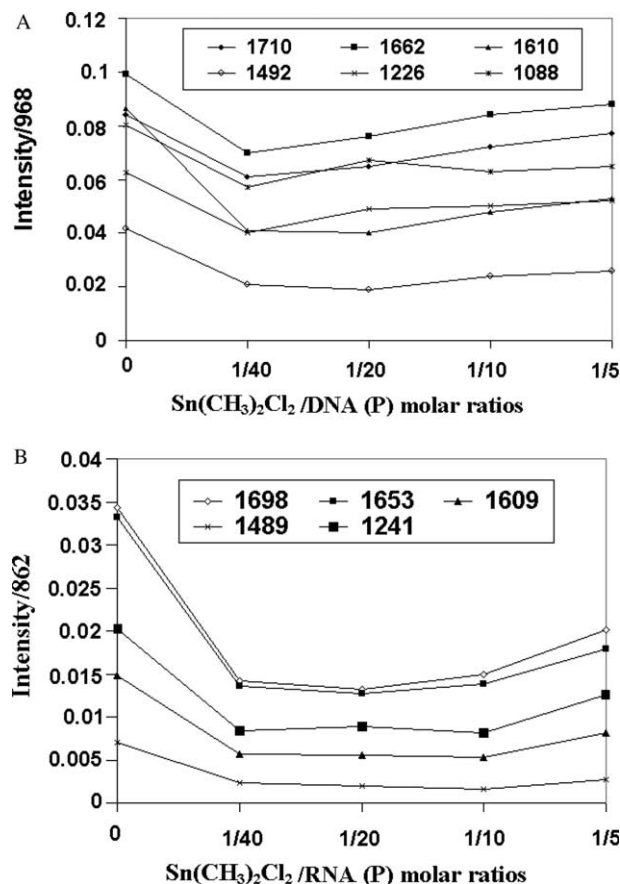


Fig. 2. Intensity ratio variations for several DNA and RNA in-plane vibrations as a function of $\text{Sn}(\text{CH}_3)_2\text{Cl}_2$ concentration. (A) Intensity ratios for the DNA bands at 1710 (G, T), 1662 (T, G, A, C), 1609 (A), 1492 (C, G), 1226 (PO_2 asymmetric stretch) and 1088 cm^{-1} (PO_2 symmetric stretch) referenced to the DNA band at 968 cm^{-1} ; (B) intensity ratios for the RNA bands at 1698 cm^{-1} (G, U), 1653 cm^{-1} (U, G, A and C; mainly uracil), 1609 cm^{-1} (A), 1489 cm^{-1} (G, C) and 1241 cm^{-1} (PO_2 stretch) referenced to RNA band at 862 cm^{-1} .

$r=1/40$) (Fig. 2A). Since, larger intensity increases were observed for the PO_2 bands at 1226 and 1088 cm^{-1} (compared with those of the bases vibrations), it is reasonable to assume that some degree of cation- PO_2 interaction occurred at higher metal ion concentrations (1/20 and 1/10). However, such interaction with phosphate group would be through OH groups of the Sn-hydroxo complexes formed in aqueous solution. As cation concentration increased ($r=1/5$), no further spectral changes observed, which is indicative of no more Sn–DNA complexation at high cation concentration (Fig. 2A).

3.2. FTIR spectra of $\text{Sn}(\text{CH}_3)_2\text{Cl}_2$ –RNA complexes

The infrared spectra of $\text{Sn}(\text{CH}_3)_2\text{Cl}_2$ –RNA adducts with various molar ratios of $\text{Sn}(\text{CH}_3)_2\text{Cl}_2$ –RNA (phosphate) were recorded. The spectral changes (intensity and shifting) of several RNA in plane vibrations at 1698 cm^{-1} (G, U; mainly guanine), 1653 cm^{-1} (U, G, A and C; mainly uracil), 1609 cm^{-1} (A), 1489 cm^{-1} (C) and 1241 cm^{-1}

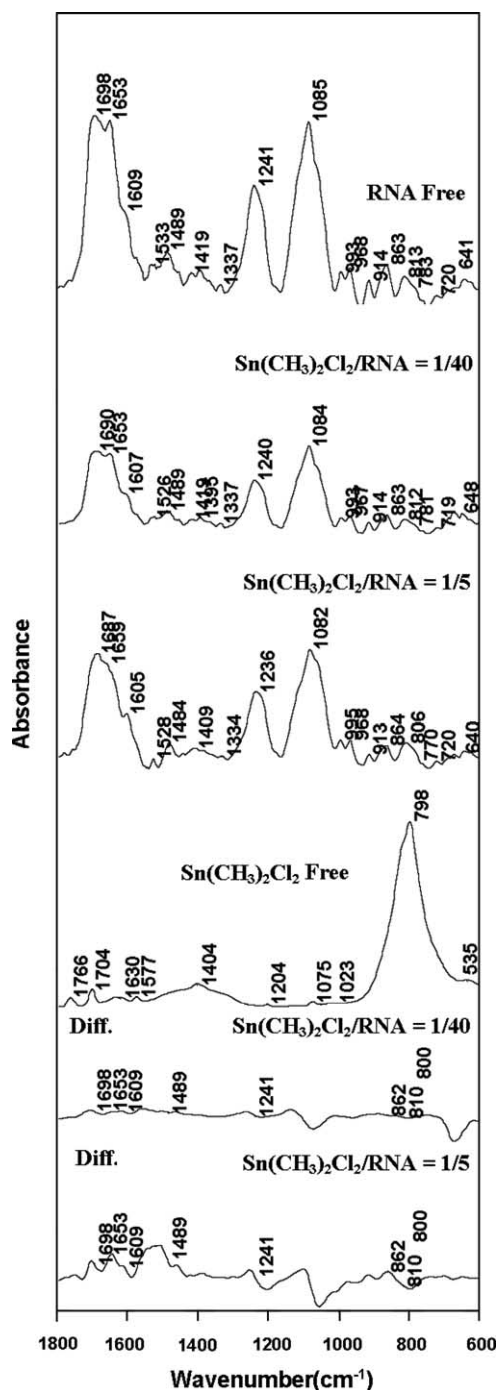


Fig. 3. FTIR spectra in the region of 1800–600 cm⁻¹ for free yeast RNA and yeast RNA, free Sn(CH₃)₂Cl₂, and Sn(CH₃)₂Cl₂-RNA adducts in aqueous solution at pH 6.5–7.5 (top four spectra) and difference spectra for Sn(CH₃)₂Cl₂-polynucleotides adducts obtained at various Sn(CH₃)₂Cl₂-RNA (phosphate) molar ratios (bottom two spectra).

(PO₂ asymmetric stretch) [21,22,30–37] were monitored at different drug concentrations (Figs. 2B and 3).

It should be noted that, Sn(CH₃)₂Cl₂ hydrolyzes in water to produce Sn(CH₃)₂(OH)₂ species that can bind indirectly to RNA bases, phosphate and deoxyribose.

At $r=1/40$, the intensity of the bands at 1698 cm⁻¹ (G) (58%), 1653 cm⁻¹ (59%), 1609 cm⁻¹ (A) (61%), 1489 cm⁻¹(C) (65%) and 1241 cm⁻¹ (PO₂) (58%) decreased, respectively, (relative to free RNA) (Fig. 2B). The major decrease in intensity can be due to RNA aggregation in the presence of organotinhydroxo complexes. The intensity variations were associated with the shift of the bands at 1698 (mainly G) to 1690 cm⁻¹, 1609 (A) to 1607 cm⁻¹ and 1241 (PO₂ stretch) to 1240 cm⁻¹ (Fig. 3). No shifting was observed for the uracil band at 1653 cm⁻¹ and cytosine band at 1489 cm⁻¹. The observed spectral changes can be due to drug interaction (indirectly) with the guanine and to a lesser extent with adenine bases (Fig. 3).

As concentration increased ($r=1/20$), no major intensity changes observed, but the guanine band at 1698 shifted to 1685 cm⁻¹ ($\Delta\nu=13$ cm⁻¹) (Fig. 3). The major shifting observed for the guanine band at 1698 cm⁻¹ is due to the Sn-RNA interaction indirectly via guanine N7 and O6. Similar spectral changes were observed in the Ag-RNA interaction [31]. At this concentration, the uracil band at 1653 shifted to 1660 cm⁻¹, adenine band at 1609 shifted to 1607 cm⁻¹ and the cytosine band at 1489 shifted to 1485 cm⁻¹. The observed spectral changes can be due to tin indirect drug interactions with G-C and A-U base pairs.

As drug concentration increased ($r=1/10$, 1/5), major increases in the intensities of RNA bands were observed in the Sn(CH₃)₂Cl₂-RNA complexes (Figs. 2B and 3). These intensity variations were also associated with the shifting of the bands at

1698 (G) to 1694 cm⁻¹ ($r=1/10$); 1687 cm⁻¹ ($r=1/5$); 1653 (U) to 1654 cm⁻¹ ($r=1/10$); 1659 cm⁻¹ ($r=1/5$); 1609 (A) to 1607 cm⁻¹ ($r=1/10$); 1605 cm⁻¹ ($r=1/5$); 1489 (C) to 1490 cm⁻¹ ($r=1/10$); 1484 cm⁻¹ ($r=1/5$); 1241 (PO₂) to 1239 cm⁻¹ ($r=1/10$); 1236 cm⁻¹ ($r=1/5$); (Fig. 3).

These spectral changes can be attributed to the Sn binding to G-C and A-U base pairs as well as PO₂ group.

3.3. DNA and RNA conformations

No conformational transition was observed in Sn(CH₃)₂Cl₂-DNA complexes. In the free DNA spectrum, the marker bands at 1710–1717 cm⁻¹ (G), 1222–1227 cm⁻¹ (asymmetric PO₂ stretching), 893 and 860 cm⁻¹ (sugar-phosphate stretching) and 836 cm⁻¹ (phosphodiester mode) (Fig. 1), are due to B-DNA conformation [38–42]. When B to A transition occurs, the DNA marker bands are shifted to 1710–1700, 1225–1240, 825–800 cm⁻¹, respectively, and a new band appears at about 870–860 cm⁻¹ [40–42]. In the B to Z conformational transition, the sugar-phosphate band at 836 cm⁻¹ appears at about 800–780 cm⁻¹, and the guanine band displaces to 1690 cm⁻¹, while the PO₂ stretching vibration shifts to 1216 cm⁻¹. Since, the sugar-phosphate

bands at 836 and 893 cm^{-1} exhibited no major shifting in the spectra of the $\text{Sn}(\text{CH}_3)_2\text{Cl}_2$ -DNA adducts, the DNA remains in the B-family structure. However, minor spectral changes (shifting and intensity changes) in the region of 1060–600 cm^{-1} of $\text{Sn}(\text{CH}_3)_2\text{Cl}_2$ -DNA complexes can be attributed to the alterations of the sugar-phosphate geometry while DNA remains in the B-family structures (Fig. 1).

RNA remains in the A-family structure in the Sn-RNA adducts. The marker bands for A-RNA conformation at 862, 810 cm^{-1} (due to ribose-phosphate vibrations), 1241 (PO_2 stretch) and 1698 (G) [42] did not show major shifting in the spectra of Sn-RNA complexes, indicating of RNA remaining in A-conformation (Fig. 3). The minor intensity variations for RNA marker bands at 862, 810 and 800 cm^{-1} are related to a perturbations of the sugar-phosphate backbone geometry upon drug interaction (Fig. 3), while RNA remains in A-conformation.

3.4. Absorption spectra of $\text{Sn}(\text{CH}_3)_2\text{Cl}_2$ -DNA complexes

The calculation of the overall binding constants were carried out using UV spectroscopy as reported.[43,44] The double reciprocal plot of $1/[\text{drug complexed}]$ vs. $1/[\text{drug}]$ is linear and the binding constant (K) is calculated from the ratio of the intercept on the vertical coordinate axis to the slope (Fig. 4). Concentrations of complexed drug were determined by subtracting absorbance of uncomplexed DNA and RNA at 260 nm from those of the complexed DNA and RNA. Concentrations of drugs were determined by subtraction of complexed drug from total drug used for the experiment. Our data of $1/[\text{drug complexed}]$ almost

proportionally increased as a function of $1/[\text{free drug}]$ (Fig. 4), and thus, the overall binding constants are estimated to be $K=1.47 \times 10^5 \text{ M}^{-1}$ for $\text{Sn}(\text{CH}_3)_2\text{Cl}_2$ -DNA and $K=7.33 \times 10^5 \text{ M}^{-1}$ for $\text{Sn}(\text{CH}_3)_2\text{Cl}_2$ -RNA complexes. The extra stability of Sn-RNA adducts ($K=7.33 \times 10^5 \text{ M}^{-1}$) over Sn-DNA complexes ($K=1.47 \times 10^5 \text{ M}^{-1}$) can be attributed to the less double helical structure of RNA, which provides greater accessibility for drug interaction with RNA bases. Similar association constants were reported for DNA and RNA complexes with AZT [20,21], Taxol [45], chlorophyll, chlorophyllin [23,25,46] and biogenic polyamines [47].

On the basis of our spectroscopic results the following conclusions are made (a) $\text{Sn}(\text{CH}_3)_2\text{Cl}_2$ hydrolysis in aqueous solution to give metal hydroxo species. (b) DNA and RNA aggregation occurred in the presence of organotin complexes. (c) Metal hydroxo complexes bind DNA mainly through the backbone phosphate group indirectly (via cation hydroxyl groups) with overall binding constant of $K=1.47 \times 10^5 \text{ M}^{-1}$. (d) RNA binding is mainly through backbone phosphate group with minor interaction with RNA bases at high drug concentration and $K=7.33 \times 10^5 \text{ M}^{-1}$. (e) The indirect cation bindings results in a partial helix stabilization with no alterations of the B-DNA or A-RNA structure.

Acknowledgements

We greatly appreciate the financial support received from AZAD university, Tehran Central Branch, Iran and Hematology, Oncology and BMT Research Center, Shariati Hospital, University of Tehran, Iran and the Natural Sciences and Engineering Research Council of Canada (NSERC).

References

- [1] A.K. Saxena, F. Huber, *Coord. Chem. Rev.* 95 (1989) 109.
- [2] M.J. Gielen, *Braz. Chem. Soc.* 14 (2003) 870.
- [3] L. Pellerito, L. Nagy, *Coord. Chem. Rev.* 224 (2002) 111.
- [4] A.J. Crowe, P.J. Smith, A. Atassi, *Chem. Biol. Interact.* 32 (1980) 171.
- [5] R. Barbieri, L. Pellerito, G. Ruisi, M.T. Lo Guidice, F. Huber, G. Attasi, *Inorg. Chim. Acta* 66 (1982) L39.
- [6] K.C. Molloy, F.R. Hartley (Eds.), *Bioorganotin Compounds: The Chemistry of Metal-Carbon Bond*, Wiley, London, 1989, p. 465.
- [7] J.M. Tsangaris, D.R. Williams, *Appl. Organomet. Chem.* 6 (1992) 3.
- [8] K. Burger, L. Nagy, K. Burger (Eds.), *Biocoordination Chemistry, Metal Complexes of Carbohydrates and Sugar-type Ligands*, Ellis Horwood, London, 1990, p. 236.
- [9] N.B. Gyurcsik, L. Nagy, *Coord. Chem. Rev.* 203 (2000) 81.
- [10] J.F. Verchere, S. Chapelle, F. Xin, D.C. Crans, *Prog. Inorg. Chem.* 47 (1998) 837.
- [11] R. Barbieri, A. Silvestri, V.J. Piro, *J. Chem. Soc., Dalton Trans.* (1990) 3605.
- [12] R. Barbieri, G. Ruisi, A. Silvestri, A.M. Giuliani, A. Barbieri, G. Spina, F. Pieralli, F. Del Giallo, *J. Chem. Soc., Dalton Trans.* (1995) 467.

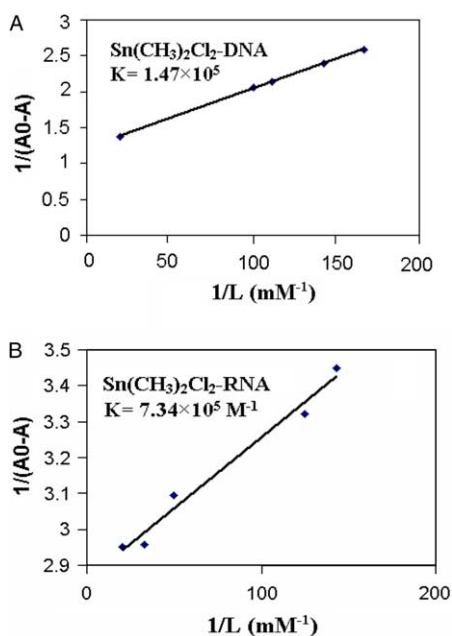


Fig. 4. The plot of $1/(A_0 - A)$ vs. $1/L$ for DNA and RNA and their drug complexes where A_0 is the initial absorption of DNA and RNA (260 nm) and A is the recorded absorption at different $\text{Sn}(\text{CH}_3)_2\text{Cl}_2$ concentrations (L).

- [13] Q. Li, P. Yang, H. Wang, M. Guo, J. Inorg. Biochem. 64 (1996) 181.
- [14] R. Barbieri, A. Silvestri, J. Inorg. Biochem. 41 (1991) 31.
- [15] R. Barbieri, A. Silvestri, A.M. Giuliani, V.J. Piro, F.D. Simone, G. Madonna, J. Chem. Soc., Dalton Trans. (1992) 585.
- [16] H. Jankovics, L. Nagy, N. Buzas, L. Pellerito, R. Barbieri, J. Inorg. Biochem. 92 (2002) 55.
- [17] G. Barone, A. Barbieri, S. Posante, A. Trotta, A. Silvestri, G. Ruisi, A.M. Giuliani, M.T. Lo Giudice, M.T. Musmeci, R.J. Barbieri, J. Inorg. Biochem. 59 (1995) 176.
- [18] A. Jansco, L. Nagy, E. Moldrheim, E. Sletten, J. Chem. Soc., Dalton Trans. (1999) 1587.
- [19] Sh. Nafisi, A. Hadjiakhoondi, A. Yektadoost, Biopolymers 74 (2004) 345.
- [20] R. Marty, A. Ahmed Ouameur, J.F. Neault, Sh. Nafisi, H.A. Tajmir-Riahi, DNA Cell Biol. 23 (2004) 135.
- [21] A. Ahmed Ouamer, R. Marty, J.F. Neault, H.A. Tajmir-Riahi, DNA Cell Biol. 23 (2004) 783.
- [22] A. Alex, P. Dupuis, Inorg. Chim. Acta 157 (1988) 271.
- [23] J.F. Neault, H.A. Tajmir-Riahi, Biophys. J. 76 (1999) 2177.
- [24] H. Arakawa, R. Ahmad, M. Naoui, H.A. Tajmir-Riahi, J. Biol. Chem. 275 (2000) 10150.
- [25] J.F. Neault, H.A. Tajmir-Riahi, J. Phys. Chem. B 102 (1998) 1610.
- [26] J.F. Neault, M. Naoui, M. Manfait, H.A. Tajmir-Riahi, FEBS Lett. 382 (1996) 26.
- [27] J.F. Neault, H.A. Tajmir-Riahi, J. Biol. Chem. 271 (1996) 8140.
- [28] J.F. Neault, M. Naoui, H.A. Tajmir-Riahi, J. Biomol. Struct. Dyn. 13 (1995) 387.
- [29] H. Arakawa, N. Watanabe, H.A. Tajmir-Riahi, Bull. Chem. Soc. Jpn. 74 (2001) 1075.
- [30] R. Ahmad, M. Naoui, J.F. Neault, S. Diamantoglu, H.A. Tajmir-Riahi, J. Biomol. Struct. Dyn. 13 (1996) 795.
- [31] H. Arakawa, J.F. Neault, H.A. Tajmir-Riahi, Biophys. J. 81 (2001) 1580.
- [32] D.E. DiRico Jr., P.B. Keller, K.A. Hartman, Nucleic Acids Res. 13 (1985) 251.
- [33] P.B. Keller, K.A. Hartman, Spectrochim. Acta, Part A 42 (1986) 299.
- [34] M. Langlais, H.A. Tajmir-Riahi, R. Savoie, Biopolymers 30 (1990) 743.
- [35] E.B. Starikov, M.A. Semenov, V.Y. Maleev, I.A. Gasan, Biopolymers 31 (1991) 255.
- [36] M. Tsuboi, Appl. Spectrosc. Rev. 3 (1969) 45.
- [37] B. Prescott, W. Steinmetz, G.J. Thomas Jr., Biopolymer 23 (1984) 235.
- [38] E. Thailandier, J. Liquier, J.A. Taboury, Advanced Infrared and Raman Spectroscopy, Wiley, New York, 1985. p. 64.
- [39] H.A. Tajmir-Riahi, J.F. Neault, M. Naoui, FEBS Lett. 370 (1995) 105.
- [40] D.M. Loprete, K.A. Hartman, Biochemistry 32 (1993) 4077.
- [41] H.A. Tajmir-Riahi, J.F. Neault, M. Naoui, S. Diamantoglou, Biopolymers 35 (1995) 493.
- [42] E. Thailandier, L. Liquier, Infrared spectroscopy of DNA, Methods Enzymol. 211 (1992) 307.
- [43] M. Klotz, D.L. Hunston, Biochemistry 10 (1971) 3065.
- [44] M. Purcell, A. Novetta-Delen, H. Arakawa, H. Malonga, H.A. Tajmir-Riahi, J. Biomol. Struct. Dyn. 17 (1999) 473.
- [45] A. Ahmed Ouameur, H. Malonga, J.F. Neault, S. Diamantoglou, H.A. Tajmir-Riahi, Can. J. Chem. 82 (2004) 1112.
- [46] R. Marty, A. Ahmed Ouameur, H.A. Tajmir-Riahi, J. Biomol. Struct. Dyn. 22 (2004) 45.
- [47] A. Ahmed Ouameur, H.A. Tajmir-Riahi, J. Biol. Chem. 279 (2004) 42041.